Physicochem. Probl. Miner. Process., 56(3), 2020, 407-420

http://www.journalssystem.com/ppmp

Physicochemical Problems of Mineral Processing

ISSN 1643-1049

Received December 23, 2020; reviewed; accepted February 26, 2020

Recovery of vanadium and tungsten from spent selective catalytic reduction catalyst by alkaline pressure leaching

Nana Liu, Xinyang Xu, and Yuan Liu

School of Resources & Civil Engineering, Northeastern University, Shenyang 110819, China

Corresponding author: xuxinyang@mail.neu.edu.cn (Xinyang Xu)

Abstract: Improving the efficiency of precious metal recovery from spent Selective Catalytic Reduction (SCR) catalyst provides economic benefits and promises sustainable use of resources. Here we demonstrate highly efficient alkaline pressure leaching method for the extraction of vanadium (V) and tungsten (W) from spent SCR catalyst. We analyzed the effects of experimental parameters such as the stirring speed, leaching agent concentration, leaching temperature, liquid-to-solid ratio, and leaching time. The Box-Behnken design of experiments and the response surface methodology have been employed to understand the impact of the leaching parameters and the impact of their interactions on the leaching rate of V and W. The results showed that the leaching agent concentration significantly promoted the recovery of V and W; the influence of the reaction temperature and leaching time moderately increased the leaching rate of the metals. Moreover, the efficiency of the alkaline pressure leaching technique was determined by the interactions between leaching time and reaction temperature, and the relationships between reaction temperature and leaching agent concentration. By using the response surface methodology, the optimal leaching conditions were found that the leaching agent concentration was 4.75 mol·L-1, the leaching temperature was 190 °C, and the reaction time was 44.5 min, and the predicted values of V and W leaching rates were 95.76% and 98.36%, respectively. Based on the excellent fitting between modeling and experimental results demonstrated in this work, we conclude that our study can shed light on the development of highly efficient and sustainable metal recovery strategies for practical applications.

***Keywords*:** spent SCR catalyst, alkaline pressure leaching, response surface method, Box-Behnken design

1. Introduction

Selective catalytic reduction (SCR) is a widely used flue gas denitrification technology in coal-fired power plants (Guo et al., 2012; Yang et al., 2013). The core of this technology involves SCR composed of metal oxides such as TiO_2, V_2O_5, and WO_3 catalyst. (Zhou et al., 2012). In the actual operation of the denitrification system, catalyst poisoning, sintering, clogging, and loss of active components lead to reduced activity and decreased lifetime of the SCR catalyst. With the large-scale construction of China's coal-fired power plants using flue gas denitrification, the amount of spent catalyst will continue to increase sharply (Shang et al., 2012; Li et al., 2014). At present, the main treatment method for spent SCR catalyst waste in China is crushing and landfill, which not only occupies land resources but also severely harms the environment. In August 2014, the Ministry of Environmental Protection of China issued the "Notice on Strengthening the Supervision of Waste Flue Gas Denitrification Catalysts" and the "Guidelines for the Examination of Hazardous Waste Business Licenses for Waste Flue Gas Denitrification Catalysts" to decontaminate waste flue gas denitrification catalysts. Therefore, the recovery of valuable metals such as vanadium (V), titanium (Ti), and tungsten (W) in the waste SCR catalyst can not only bring significant economic benefits but also avoid environmental pollution and waste of resources (Perez et al., 2019; Marafi et al., 2008).

DOI: 10.37190/ppmp/118475

The recovery processes of valuable metals in spent SCR catalyst waste mainly include sodium roasting, acid leaching, and alkali leaching (Li et al., 2014; Marafi and Stanislaus, 2008; Tuncuk et al., 2009; Huo et al., 2015). Generally, the sodium roasting process involves recurring calcination steps at high temperature; therefore, it requires specialized equipment causing high energy consumption (Li et al., 2015). Moreover, exhaust gas released during the process aggravates the environmental burden (Li et al., 2017). On the other hand, the acid leaching processes consume a tremendous amount of acid and generate a large amount of wastewater as well as impurities (Borra et al., 2016; Ku et al., 2016). As opposed to the high energy consumption of the sodium roasting process and the low leaching rate of the acid leaching process, the advantages of the alkali leaching process is promising for efficient treatment of the spent SCR catalyst (Fan et al., 2013; Kim et al., 2015). Conventional alkali leaching processes mainly include atmospheric pressure alkali leaching, Na_2CO_3 high-pressure leaching, and NaOH pressure leaching. Pressure leaching with NaOH offers low alkali concentration, short leaching time, low energy consumption, and high leaching rate, and thus has broad industrial application prospects. However, previous studies on the recovery of valuable metals via alkaline pressure leaching from spent SCR catalyst are limited to the investigation of only single factor influence on the leaching rate; thus, systematic and comprehensive analysis of various acting factors as well as the impact of their interactions, on leaching efficiency is required.

Response surface methodology (RSM) is an experimental design optimization method commonly used in multi-factor systems (Khuri and Mukhopadhyay, 2010; Myers et al., 2016). RSM combines mathematical and statistical analysis, uses multiple quadratic linear regression techniques to solve multivariate equation problems, and establishes a continuous variable surface model. Through the analysis of multi-functional response surfaces and contours, the interaction between influential factors can be determined using RSM (Makadia and Nanavati, 2013; Shi et al., 2018). The response surface method is advantageous compared with the single-factor experiment and the orthogonal test method since it can quickly and effectively help determine the optimal control conditions of the multi-factor system, the primary and secondary relationships of various process parameters, and the interaction between specific factors (Kenné, 1999; Gharbi and Kenné, 2000). Design methods such as Box-Behnken (BBK) and Central Composite Design (CCD) have been widely used in various fields such as pharmaceutical science, geology, food science, metallurgy, and materials for experimental optimization (Solanki, et al., 2007; Tefas et al., 2015; Muthukumar et al., 2003; White et al., 2001; Tekindal et al., 2012).

In this study, V and W were recovered by pressure leaching with NaOH from the spent SCR catalyst. The single-factor experimental method was used to investigate the influence of stirring speed, leaching agent concentration, reaction temperature, liquid-to-solid ratio, and leaching time on the leaching rate of V and W. The main factors and levels affecting the leaching rate of V and W were identified for modeling. Based on the Box-Behnken (BBK) experimental design, the response surface method was used to optimize the alkali leaching conditions for optimal recovery of V and W from the spent SCR catalyst.

2. Materials and methods

2.1. Raw materials and their characterization

The honeycomb SCR catalyst (vanadium and titanium) discarded by a domestic thermal power plant was used. The sample was a light yellow powder with fine particle size. The chemical composition was analyzed by XRF-1800 fluorescence spectrometer (XRF) (Shimadzu, Japan), as shown in Table 1.

Table 1. Composition of the spent SCR catalyst

Composition	TiO_2	SiO_2	WO_3	CaO	Al_2O_3	S	V	MgO	P
Content/wt. %	82.28	4.28	3.93	1.36	0.81	0.48	0.40	0.17	0.03

The size distribution of samples were analyzed using a Mastersizer2000 laser particle sizer (Malvern Instruments Co., Ltd., UK). The cumulative particle size distribution is shown in Fig. 1. Particles with an average size of 28.47 μm accounted for 90%; those with an average size of 0.24 μm accounted for only

0.02% of all. The d90, d50, and d10 diameters are 25, 10, 0.83 μm, respectively. In the experiment, 0.22 μm polytetrafluoroethylene (PTFE) filter membrane was used for the extraction filtration of the reaction solution to ensure that all the leaching residue was retained on the membrane.

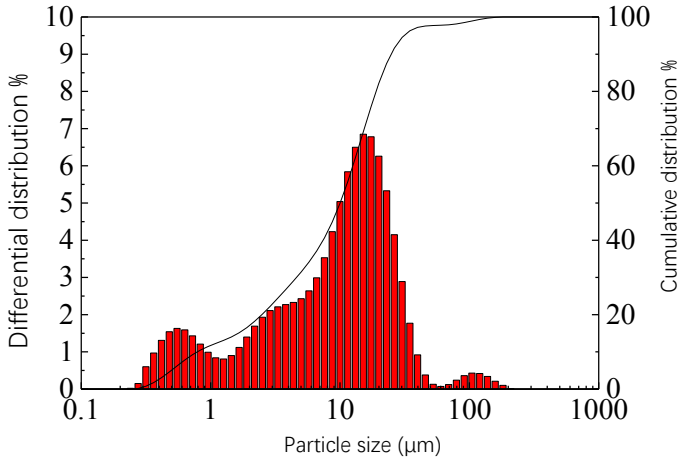

Fig. 1. Particle size distribution of the spent SCR catalyst

2.2. Alkaline leaching

The YZPR-100 type reactor (Shanghai Yanzheng Test Instruments Co., Ltd., China) was used to inject a certain amount of water into its matching 100 ml PTFE beaker. After the reactor cover was tightened, the temperature was kept at 180 °C for 2 h. The reactor was used in the airtight condition indicated by no further change in pressure. Then, the spent SCR catalyst powder and NaOH solution were added to a PTFE beaker at a specific ratio, stirred evenly, and placed in the high-pressure reactor after sealing with a cover. After the temperature raised to the set temperature, the stirring was started, and the air was pumped in, and the leaching time was initiated. After the leaching was completed and cooled, the pressure was removed, and the reactor was opened. The reaction solution was taken out, washed with distilled water; then, the supernatant was vacuum-filtrated through a 0.22 μm PTFE filter membrane; the solid phase was washed and filtered. After triple washing with distilled water of the same volume, the leaching residue was obtained. The leaching residue was then put into the WGL-65B type electric blast drying oven (Tianjin Taisite Instrument Co., Ltd., China), dried, weighed, and analyzed by XRF. The V and W leaching rates, η_V and η_W, were calculated based on the detection results of the leaching residue. The calculation formulas are as follows:

$$\eta_v = \left(1-\frac{m_1 \times w_{V1}}{m_0 \times w_{V0}}\right) \times 100\% \quad (1)$$

$$\eta_w = \left(1-\frac{m_1 \times w_{W1}}{m_0 \times w_{W0}}\right) \times 100\% \quad (2)$$

where η_V and η_W are the leaching rates (%) of V and W in the leaching process, m_0 and m_1 are the masses (g) of the original sample and the leaching residue, w_{V0} and w_{W0} are the mass fractions (%) of V and W in the original sample, and w_{V1} and w_{W1} are the mass fractions (%) of V and W in the leaching residue, respectively.

2.3. Single-factor experimental design

NaOH was used as the leaching agent for the recovery of V and W from the spent SCR catalyst. The effects of agitation speed, NaOH concentration, reaction temperature, liquid-to-solid ratio, and leaching time on the leaching rates of V and W were investigated. The main influential factors, as well as the optimal range of each factor, were determined.

2.4. Response surface optimization design

According to the single-factor experimental results (Section 3), the fixed agitation speed was 600 r/min, and the liquid-to-solid ratio was 10:1. Three factors that had a great influence on the leaching rates of V

and W were selected as the experimental variables: leaching agent concentration (X_1), reaction temperature (X_2), and leaching time (X_3). Note the liquid-to-solid ratio had a minimal effect on the leaching rates of V and W, as shown in Fig.5. The leaching rates of V and W were taken as the response values, which were represented by Y_1 and Y_2, respectively. The Dedign-Exoert8.0.6 software, based on the Box-Behnken experimental principle, was used to design an experimental optimization scheme of three factors and three levels. The experimental results were optimized and analyzed. The experimental factors and levels are shown in Table 2. In this experiment, the quadratic polynomial was used to fit the experimental data (Ooi et al., 2018; Zi et al., 2013):

$$Y = \beta_0 + \sum_{i=1}^{3} \beta_i X_i + \sum_{i=1}^{3} \beta_{ii} X_i^2 + \sum_{i=1}^{3} \beta_{ij} X_i X_j + \epsilon \quad (3)$$

where Y is the response value, X_i is the independent variable, β_0 is the response model constant, β_i is the linear parameter coefficient, β_{ii} is the quadratic parameter coefficient, β_{ij} is the interaction parameter coefficient, and ϵ is the error.

Table 2. Independent variables and their levels in the Box-Behnken design

Factor	Code	Level (x_i)		
		-1	0	+1
Leaching agent concentration (mol·L^{-1})	X_1	1	3	5
Reaction temperature (℃)	X_2	110	150	190
Leaching time (min)	X_3	30	90	150

3. Results and discussion

3.1. Single-factor experimental results

3.1.1. The effect of agitation speed on the leaching rates of V and W

Fig. 2 shows the effect of agitation speed on the leaching rates of V and W when the NaOH concentration was 1 mol·L^{-1}, the liquid-to-solid ratio was 10:1, the leaching temperature was 110 ° C, the leaching pressure was equal to the vapor pressure at around 0.1 Mpa, and the leaching time was 30 min. The results show that the leaching rates of V and W gradually increased with the increase of agitation speed and remained nearly the same above 600 r·min^{-1}. Upon the increase of the agitation speed to a certain intensity, the reaction solution is mixed evenly, and the mass transfer resistance outside the particles decreases correspondingly, thereby increasing the leaching rates of V and W (Skelland and Li, 1981). When the agitation speed was 600 r·min^{-1}, the leaching rates of V and W reached 86.8% and 77.8%, respectively; they changed little with further increasing the agitation speed. This result is in line with the typical influence of the leaching kinetics on the leaching efficiency reported elsewhere (Chen et al., 2013; Liu et al., 2014). Therefore, 600 r·min^{-1} was selected as the optimal agitation speed to eliminate the impact of external diffusion on the leaching rate.

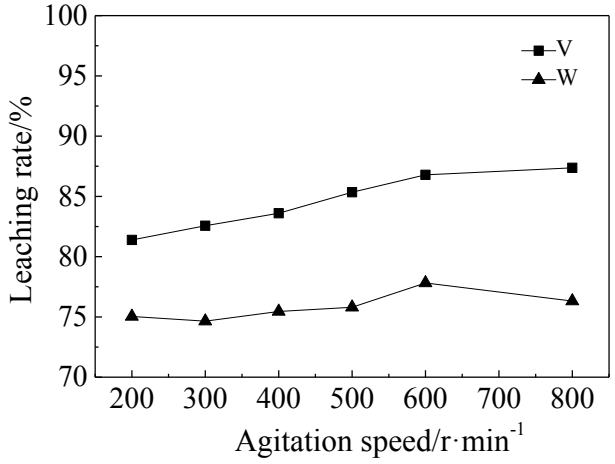

Fig. 2. The effect of agitation speed on the leaching rates of V and W

3.1.2. The effect of NaOH concentration on the leaching rates of V and W

NaOH was used as the leaching agent to perform the alkaline pressure leaching on the spent SCR catalyst. The agitation speed was 600 r·min^{-1}, the liquid-to-solid ratio was 10:1, the leaching temperature was 110 ℃, the leaching pressure was same as the vapor pressure at around 0.1 Mpa, and the leaching time was 30 min. Fig. 3 shows that the leaching rates of V and W increased significantly with the increase of NaOH concentration. When the NaOH concentration was 0.5 mol · L^{-1}, V reacted preferentially with NaOH because of its high reactivity, and its leaching rate was 87.0%. With the increase of the leaching agent concentration, the leaching rate of W increased rapidly; but the leaching rate of V showed a downward trend because the increased NaOH reacts with a relatively larger amount of W; the rapid decrease in the leaching agent concentration leads to a decrease in the leaching rate of V. When the NaOH concentration was greater than 4 mol · L^{-1}, the leaching rates of V and W have remained nearly the same. Excess alkali can promote the precipitation of impurity elements and increase the residual amount of alkali in the reaction solution, thereby aggravating the difficulty of subsequent purification and impurity removal (Kim et al., 2015); therefore, 4 mol · L^{-1} NaOH was optimal for the leaching of V and W.

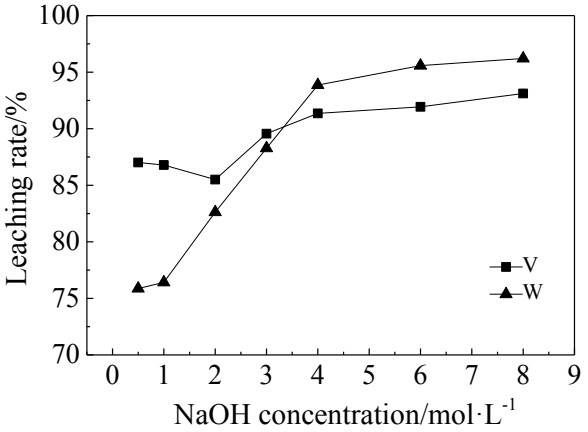

Fig. 3. The effect of NaOH concentration on the leaching rates of V and W

3.1.3. The effect of leaching temperature on the leaching rates of V and W

Temperature is one of the most critical factors affecting the metal leaching rate (Qiu et al., 2011; Angelidis et al., 1995). The effect of leaching temperature on the leaching rates of V and W were investigated under the following conditions: the agitation speed was 600 r·min^{-1}, the leaching pressure was same as the vapor pressure from around 0.1 MPa to 1.2 Mpa, the NaOH concentration was 4 mol·L^{-1}, the liquid-to-solid ratio was 10:1, and the leaching time was 30 min. The results are shown in Fig. 4. With the increase of the reaction temperature, the reaction rate increases, and the leaching rates of both V and W gradually increase. When the temperature was 150 °C, the leaching rates of V and W reached 94.3% and 95.0%, respectively. When the temperature was 170 ℃, the leaching rate of V rapidly decreased from 94.3% to 92.8%. As the temperature continued to rise, the leaching rate of V tended to be the same, while the leaching rate of W increased with the increase of temperature. Because extremely high temperatures cause the vapor pressure in the autoclave to rise sharply, considering safety and energy consumption, we found that the optimal leaching temperature should be 150 °C.

3.1.4. The effect of liquid-to-solid ratio on the leaching rates of V and W

Fig. 5 shows the effect of liquid-to-solid ratio on the leaching rates of V and W. The leaching pressure was equal to the vapor pressure at around 0.3 MPa, the NaOH concentration was 4 mol·L^{-1}, the leaching temperature was 150 ℃, the agitation speed was 600 r·min^{-1}, and the leaching time was 30 min. As shown in Fig. 5, with the increase of liquid-to-solid ratio, the leaching rate of V first increased and then decreased, while the leaching rate of W gradually increased and remained unchanged. When the liquid-to-solid ratio was relatively low, the viscosity of the reaction solution was unconducive to diffusion, thereby affecting the progress of the leaching process and resulting in a low metal leaching rate (Li et

al., 2010). With the increase of liquid-to-solid ratio, the reaction solution gradually became thinner, and the leaching agent content increased; as a result, both the leaching rates of V and W increased. When the liquid-to-solid ratio was 10:1, the leaching rates of V and W reached 94.3% and 95.0%, respectively. The leaching rates of V and W remained nearly the same above 10:1 liquid-to-solid ratio; thereby, it was found to be optimal for the alkali leaching of V and W.

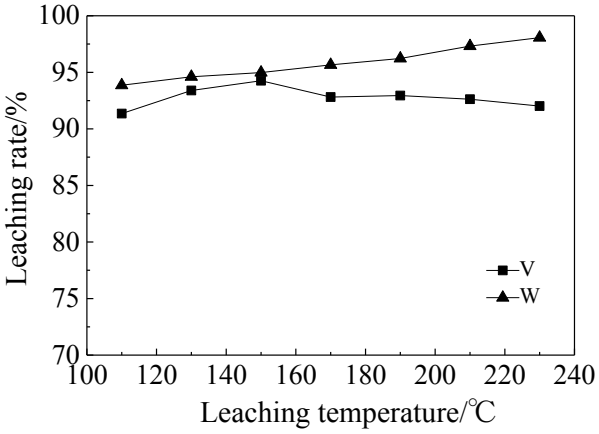

Fig. 4. The effect of leaching temperature on the leaching rates of V and W

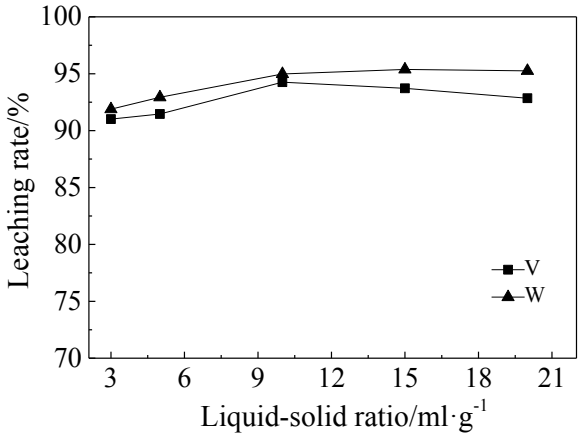

Fig. 5. The effect of liquid-to-solid ratio on the leaching rates of V and W

3.1.5. The effect of leaching time on the leaching rates of V and W

Fig. 6 shows the effect of leaching time on the leaching rates of V and W under the following conditions: the vapor pressure was used as leaching pressure at around 0.3 MPa, the NaOH concentration was 4 mol·L-1, the liquid-to-solid ratio was 10:1, the leaching temperature was 150 ℃, and the agitation speed was 600 r·min-1. As shown in Fig. 6, the leaching rates of V and W first increased and then remained stable with the extension of leaching time. When the leaching time was 2 min, both the leaching rates of V and W were high because the leaching reaction had started during the heating process of the reactor; the metal had completed partial leaching when the specified temperature was reached. When the leaching time was 60 min, the leaching rates of V and W reached 95.6% and 95.3%, respectively. When the leaching time continued to increase to 120 min, the leaching rate of V decreased significantly, while the leaching rate of W continued to increase slowly. The optimal leaching time was determined as 60 min.

3.2. Response surface optimization

3.2.1. The response surface method

According to the single-factor alkaline leaching experiments, leaching agent concentration, reaction

temperature, and leaching time were determined to be the most influential factors on the leaching rate of V and W. Therefore, these three factors were selected as the experimental variables, and the leaching rates of V and W were used as the response values. The three-factor and three-level optimization schemes were designed by Box-Behnken. Seventeen experimental points were generated by the Design Expert (version 8.0.6) software. The experimental and predicted values of V and W leaching rates under various experimental conditions are shown in Table 3.

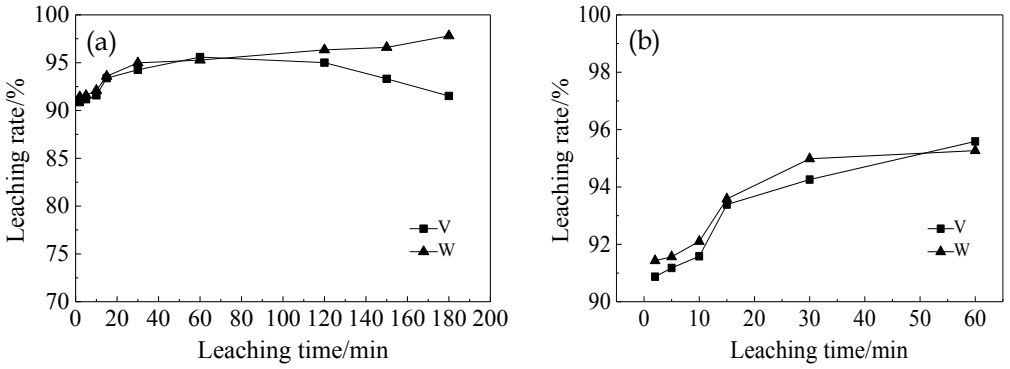

Fig. 6. a) The effect of leaching time on the leaching rates of V and W b) Zoomed in for the first 60 min

Table 3. Experimental design and results table

Standard order	NaOH concentration /(mol·L^{-1})	Leaching temperature /℃	Leaching time /min	Leaching rate of V /%		Leaching rate of W /%	
				Actual	Predicted	Actual	Predicted
1	3.00	150.00	90.00	92.7	92.43	91.72	91.42
2	5.00	190.00	90.00	95.83	95.32	98.16	97.87
3	3.00	110.00	150.00	91.42	90.25	90.95	90.05
4	1.00	150.00	30.00	90.28	89.64	80.45	80.14
5	3.00	150.00	90.00	92.79	92.43	91.14	91.42
6	5.00	150.00	150.00	89.79	90.43	96.82	97.13
7	1.00	150.00	150.00	85.1	85.76	82.7	83.31
8	3.00	190.00	150.00	90.03	89.91	95.84	95.82
9	1.00	110.00	90.00	88.5	89.01	76.1	76.39
10	3.00	150.00	90.00	92.42	92.43	91.32	91.42
11	3.00	150.00	90.00	92.04	92.43	91.33	91.42
12	1.00	190.00	90.00	92.2	91.67	85.52	84.93
13	3.00	150.00	90.00	92.19	92.43	91.57	91.42
14	5.00	150.00	30.00	92.28	91.62	96.63	96.02
15	3.00	190.00	30.00	94.6	95.77	93.64	94.54
16	3.00	110.00	30.00	89.34	89.47	87.02	87.04
17	5.00	110.00	90.00	91.48	92.01	92.57	93.16

The response surface method mainly includes first-order (linear), two-factor interaction (2FI), second-order, and third-order models (quadratic model); the summary of the models is shown in Table 4. The leaching rates of V and W are suitable to adopt the second-order model. To determine the authenticity of the fitting model, we analyzed the numerical values of the model's multiple correlation coefficient R^2 and the adjusted determination coefficient R^2_{adj}. The multiple correlation coefficient of the regression equation for the V leaching rate was $R^2 = 0.9374$, and its adjusted determination coefficient was $R^2_{adj} = 0.8568$, whereas for the W leaching rate, the multiple correlation coefficient of the regression equation was $R^2 = 0.9859$, and its adjusted determination coefficient was $R^2_{adj} = 0.9938$. The value of the multiple correlation coefficient nearing 1 indicates that it is reasonable to adopt the second-order model for the leaching of V and W. The standard deviations (Std. Dev.) were 0.92 and 0.72, respectively, further indicating that the experimental error was small and the second-order model had an excellent fit for V

and W leaching (Mirazimi et al., 2013).

Table 4. Model summary statistics

	Model	Standard deviation (Std. Dev.)	Multiple correlation coefficient (R^2)	Adjusted determination coefficient (Adj.R^2)	Remark
Vanadium	Linear	1.80	0.5555	0.4529	
	2FI	1.71	0.6920	0.5072	
	Quadratic	0.92	0.9374	0.8568	Suggested
Tungsten	Linear	1.96	0.9153	0.8958	
	2FI	2.11	0.9246	0.8794	
	Quadratic	0.72	0.9938	0.9859	Suggested

Using the Design Expert software, we fitted the data in Table 4 with multiple quadratic regression models, and the multiple regression model equations of response values and variables were obtained by:

$$Y_1 = 92.43 + 1.66\,X_1 + 1.49\,X_2 - 1.27\,X_3 + 0.16\,X_1X_2 + 0.67\,X_1X_3 - 1.66\,X_2X_3 - 1.21\,X_1^2 + 0.78\,X_2^2 - 1.86\,X_3^2 \quad (5)$$

$$Y_2 = 91.42 + 7.43\,X_1 + 3.32\,X_2 + 1.07\,X_3 - 0.96\,X_1X_2 - 0.52\,X_1X_3 - 0.43\,X_2X_3 - 3.02\,X_1^2 - 0.31\,X_2^2 + 0.75\,X_3^2 \quad (6)$$

where Y_1 is the leaching rate (%) of V, Y_2 is the leaching rate (%) of W, X_1 is the leaching agent concentration (mol·L^{-1}), X_2 is the reaction temperature (°C), and X_3 is the leaching time (min).

3.2.2. Analysis of variance (ANOVA)

To model V and W leaching rates and the significance of its influential factors, we conducted Pareto analysis of variance (ANOVA), as shown in Tables 5 and 6. The model accuracy and the significance of each influential factor were determined by F value and P value. When F value increases and P value decreases, the model accuracy improves or the factor on the response value reveals more influential. When $P \le 0.05$, it is considered a significant term; when $P \le 0.01$, it is assumed a highly significant term; and when $P \le 0.001$, it is deemed an extremely significant term.

Table 5 Analysis of variance (ANOVA) for the V leaching rate

Source	Coefficient estimate	Sum of squares	Degree of freedom	Mean square	F value	Probability (P value)
Model	92.43(intercept)	89.06	9	9.90	11.64	0.0019
X_1	1.66	22.11	1	22.11	26.01	0.0014
X_2	1.49	17.76	1	17.76	20.89	0.0026
X_3	-1.27	12.90	1	12.90	15.18	0.0059
X_1X_2	0.16	0.11	1	0.11	0.12	0.7349
X_1X_3	0.67	1.81	1	1.81	2.13	0.1880
X_2X_3	-1.66	11.06	1	11.06	13.00	0.0087
X_1^2	-1.21	6.12	1	6.12	7.19	0.0314
X_2^2	0.78	2.56	1	2.56	3.01	0.1263
X_3^2	-1.86	14.57	1	14.57	17.14	0.0043
Residual		5.95	7	0.85		
Lack of fit		5.54	3	1.85	17.91	0.0088
Pure error		0.41	4	0.10		
Corrected total		95.01	16			
C.V. (%)	1.01					
Adeq. precision	14.158					

Table 5 shows that the F value of the V leaching rate model was 11.64, and the P value was 0.0019 ($P < 0.01$), indicating that the model had high accuracy, and the influential factors had a nonlinear relationship with the V leaching rate. In this model, the influential factors of one-degree term X_1

(leaching agent concentration), X_2 (reaction temperature), X_3 (leaching time), the interaction term X_2X_3, and the quadratic term X_3^2 had a highly significant impact on the V leaching rate, while the quadratic term X_1^2 had a significant impact on the V leaching rate, and the other terms were insignificant. Thus, the order of significance on the leaching rate of V was concluded as $X_1 > X_2 > X_3^2 > X_3 > X_2X_3$, while the order of significance for the interaction terms was $X_2X_3 > X_1X_3 > X_1X_2$. The sign of the interaction term coefficient shows that synergistic effect takes place for the interaction terms X_1X_2 and X_1X_3, while the interaction effect is antagonistic for X_2X_3.

Table 6. Analysis of variance (ANOVA) for the W leaching rate

Source	Coefficient estimate	Sum of squares	Degree of freedom	Mean square	*F* value	Probability (*P* value)
Model	91.42(intercept)	584.47	9	64.94	125.61	< 0.0001
X_1	7.43	441.19	1	441.19	853.33	< 0.0001
X_2	3.32	87.91	1	87.91	170.04	< 0.0001
X_3	1.07	9.18	1	9.18	17.76	0.004
X_1X_2	-0.96	3.67	1	3.67	7.09	0.0323
X_1X_3	-0.52	1.06	1	1.06	2.05	0.1951
X_2X_3	-0.43	0.75	1	0.75	1.45	0.2681
X_1^2	-3.02	38.41	1	38.41	74.3	< 0.0001
X_2^2	-0.31	0.4	1	0.4	0.77	0.4086
X_3^2	0.75	2.4	1	2.4	4.64	0.0683
Residual		3.62	7	0.52		
Lack of fit		3.41	3	1.14	21.76	0.0061
Pure error		0.21	4	0.052		
Corrected total		588.09	16			
C.V. (%)	0.80					
Adeq precision	38.954					

Table 6 shows the F value of the W leaching rate model was 125.61, and the P value was <0.0001, indicating the model is extremely significant at a 99% confidence level. In this model, the influential factors of one-degree term X_1 (leaching agent concentration), X_2 (reaction temperature), and quadratic term X_1^2 had an extremely significant impact on the W leaching rate; the one-degree term X_3 (leaching time) had a highly significant impact on the W leaching rate; the interaction term X_1X_2 had a significant impact on the W leaching rate; and the other terms were insignificant. The significance order of the influential factors was found as $X_1 > X_2 > X_1^2 > X_3 > X_1X_2$, and $X_1X_2 > X_1X_3 > X_2X_3$ for the interaction terms. From the sign of the interaction term coefficient, we conclude that the interaction terms X_1X_2, X_1X_3, and X_2X_3 have an antagonistic effect.

Tables 5 and 6 show that the coefficients of variation (C.V. (%)) of the V and W leaching rate models were 1.01 and 0.80, respectively. The small coefficient of variation indicates high accuracy and reliability. Adeq. precision, also known as signal-to-noise ratio (SNR), is usually greater than 4. Both the V and W leaching rate models had relatively high signal-to-noise ratios, 14.158 and 38.954, respectively. with the increase of the values, the model's fitting, repeatability, and applicability become better.

The reliability analysis of the regression equations of the V and W leaching rates was carried out to further verify the feasibility of the model. The linear relationship between the predicted and experimental values of the V and W leaching rates is shown in Fig. 7. The experimental values were evenly distributed close to the straight line, indicating that the model can accurately represent the experimental data, thereby proving the rationality and effectiveness of the regression models for V and W leaching.

3.2.3. Factor interaction analysis

The response surface is a three-dimensional map obtained by fixing one factor and the other two factors

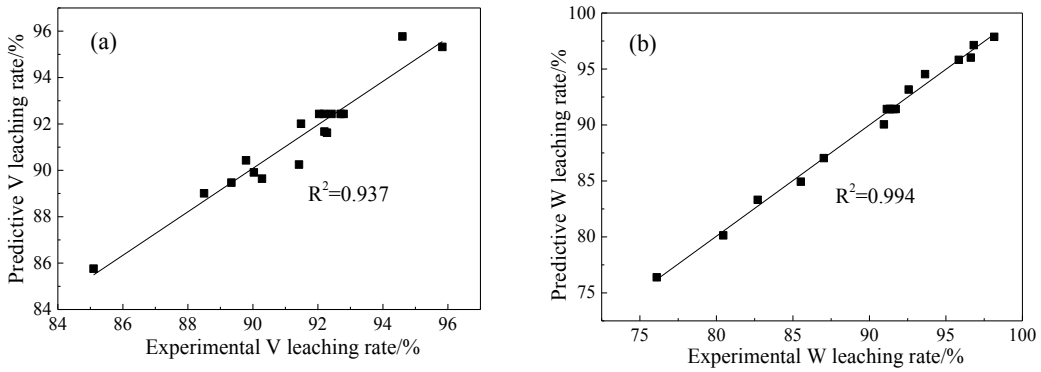

Fig. 7. Comparison of predicted and experimental leaching rates: (a) V leaching rate; (b) W leaching rate

and response values as X, Y, and Z axes, respectively; the corresponding contour map is the projection of the curve of the response value on the XY plane of the three-dimensional map (Myers et al., 2016). The response surface map and the contour map can visually reflect the influence of various factors on the leaching rate of V and W and the degree of interaction between the factors. With the increase of the slope of the response surface, the influence of the factor on the response value becomes greater. When the contour map is elliptical, it indicates that the interaction between the factors is significant, whereas when it is circular, the interaction is insignificant.

The response surface and contour plots of V leaching rate and W leaching rate are shown in Figs. 8 and 9. Fig. 8a shows that when the leaching time was fixed at 90 min, the V leaching rate increased with

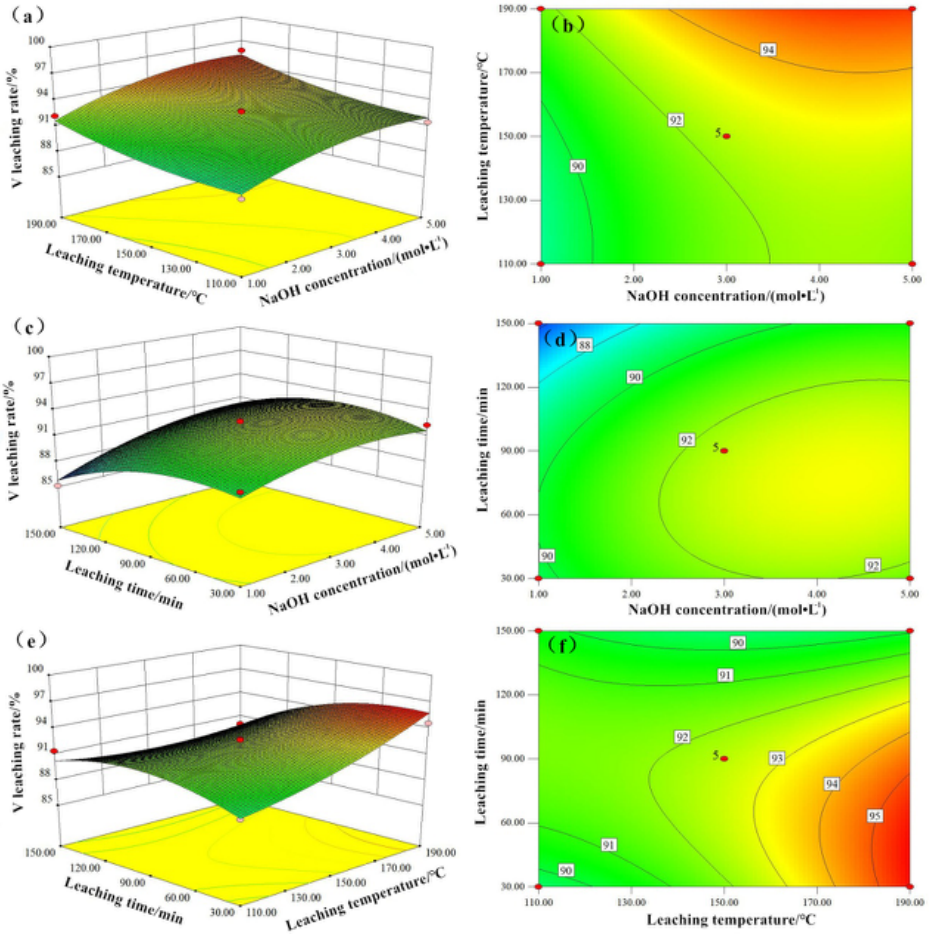

Fig. 8. Response surface and contour plots for V leaching: (a) Factor X1-X2 response surface, (b) Factor X1-X2 contour map, (c) Factor X1-X3 response surface, (d) Factor X1-X3 contour map, (e) Factor X2-X3 response surface, and (f) Factor X2-X3 contour map

the leaching temperature and the leaching agent concentration. Increasing the temperature and alkali concentration accelerates the dissolution of V; but when the concentration of NaOH is more than 4 mol·L^{-1}, the leaching rate of V remains the same, and the concentration of lye will be excessively precipitated, and the alkali consumption will increase. Therefore, the leaching agent concentration should be accordingly reduced. The response surface is hyperbolic, and the curve corresponding to the leaching temperature is relatively steep, indicating that leaching temperature has a greater influence on V leaching rate than leaching agent concentration. The contours shown in Fig. 8b indicate that the interaction between the leaching temperature and the leaching agent concentration is insignificant.

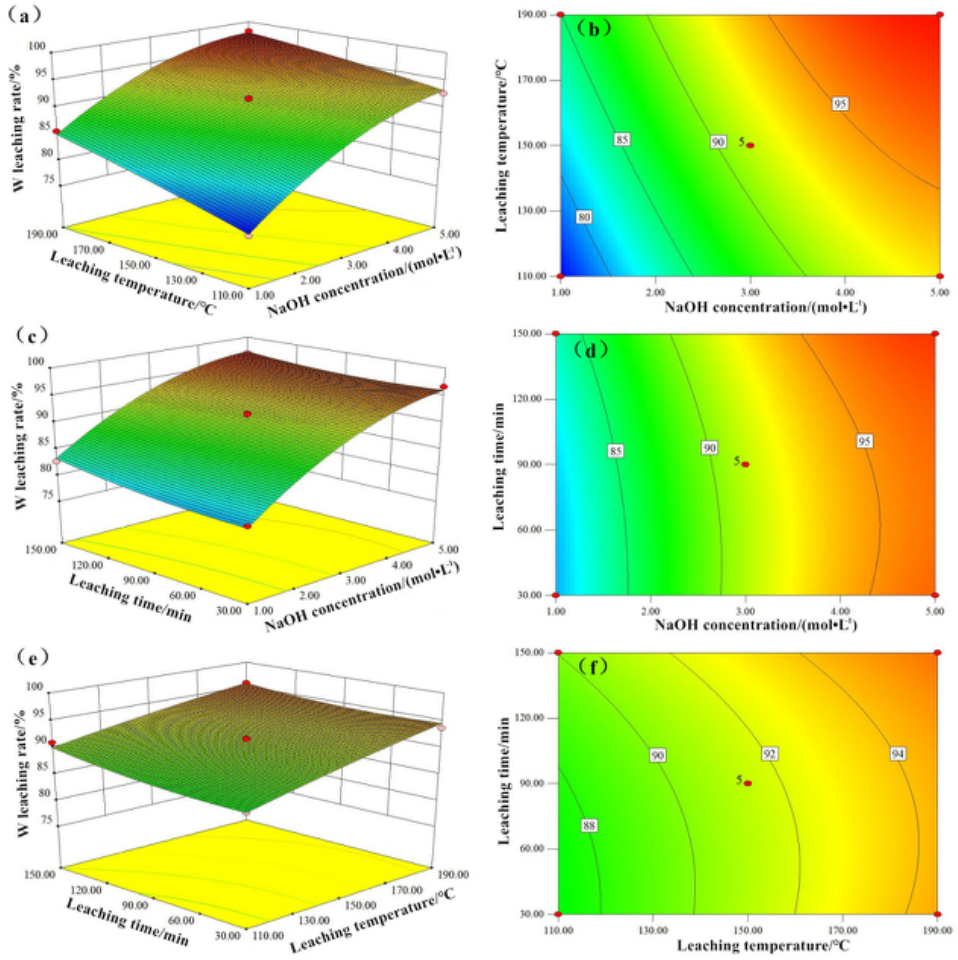

Fig. 9. Response surface and contour plots for W leaching: (a) Factor X1-X2 response surface, (b) Factor X1-X2 contour map, (c) Factor X1-X3 response surface, (d) Factor X1-X3 contour map, (e) Factor X2-X3 response surface, and (f) Factor X2-X3 contour map

Fig. 8c shows the response surface of the interaction between the reaction time and leaching agent concentration on the V leaching rate. When the reaction temperature remains 150 °C, the bending of the response surface is apparent. With the increase of reaction time, the V leaching rate increases first and then decreases. The concentration of the leaching agent has no significant effect on the V leaching rate. When the reaction time was 76 min and the leaching agent concentration was 4.25 mol·L^{-1}, the V leaching rate reached a maximum of 93.09%. The profile of the contour plot (Fig. 8d) is close to a circle, indicating that the interaction between the leaching temperature and the leaching agent concentration is insignificant.

Fig. 8e is the response surface of the interaction of reaction time and leaching temperature on V leaching rate. When the concentration of the leaching agent was fixed at 3 mol·L^{-1}, the V leaching rate increased little with the increase of the reaction time. The curve corresponding to the leaching temperature showed a linear upward trend, indicating that the increase of the leaching temperature greatly accelerated the reaction of V and NaOH and promoted the increase of the V leaching rate. The

contour plot (Fig. 8f) shows that the outline is elliptical, which indicates the interaction between the leaching temperature and the leaching agent concentration is significant.

The order of influence of the three factors on the V leaching rate is concentration of leaching agent, reaction temperature, and leaching time. The influence of interaction between two factors on V leaching rate is in the order of reaction time and leaching temperature > reaction time and concentration of leaching agent > leaching temperature and concentration of leaching agent. These results were consistent with the difference analysis in Table 5.

Fig. 9a is the response surface of the interaction between leaching temperature and leaching agent concentration on the W leaching rate. When the leaching time was fixed at 90 min, the response surface was more curved, and the leaching temperature and the leaching agent concentration increased the W leaching. Both had a large promoting effect; the increase in the leaching agent concentration significantly accelerated the dissolution of the W phase and had a significant effect on the W leaching rate. The contour plot (Fig. 9b) shows that the outline is elliptical, indicating that the interaction between leaching temperature and leaching agent concentration is significant.

Fig. 9c is the response surface of the interaction of reaction time and leaching agent concentration on the leaching rate of W. When the fixed reaction temperature was 150 °C, the leaching rate of W increased slowly with the increase of reaction time, whereas the concentration of the leaching agent increased. This result indicates that the interaction of reaction time and leaching agent concentration has a great influence on W leaching. The contour plot (Fig. 9d) shows that the interaction between leaching time and leaching agent concentration is insignificant.

Fig. 9e is the response surface of the interaction between reaction time and leaching temperature on the leaching rate of W. When the leaching agent concentration was fixed at 3 mol·L^{-1}, the slope of the response surface was slow, and the reaction time and leaching temperature increased for W leaching. The effect of the rate is not apparent; but the effect of the leaching temperature is higher than the reaction time. The contour plot (Fig. 9f) shows that the contour is nearly circular, indicating that the interaction between the leaching temperature and the leaching agent concentration is insignificant.

The order of influence of the three factors on the W leaching rate is leaching agent concentration, reaction temperature, and leaching time. The influence of interaction between two factors on W leaching rate is in the order of leaching temperature and concentration of leaching agent > reaction time and concentration of leaching agent > reaction time and leaching temperature. These results were consistent with the difference analysis in Table 6.

3.2.4. Process parameter optimization and verification experiment

According to the response surface model established above, the model was optimized by the Design Expert software. The optimal conditions for the V and W leaching in the spent SCR catalyst were achieved for the leaching agent concentration of 4.75 mol·L^{-1}, leaching temperature of 190 °C, and a reaction time of 44.5 min. Under these conditions, the leaching rates of V and W were predicted to reach 96.08% and 98.06%, respectively. To verify the optimal experimental parameters predicted by the response surface model, we carried out three verification experiments under the optimal process conditions. During the experiments, other experimental conditions were fixed at a stirring speed of 600 r·min^{-1} and the liquid-to-solid ratio of 10:1. The V leaching rates were found as 95.74%, 95.91%, and 95.63% for which the average value was 95.76% and the relative error was 0.33%. The W leaching rates were 98.36%, 98.70%, and 98.82%, respectively. The average value of the W leaching rate was 98.63% with a relative error of 0.58%. These results further indicate that this model predicts the leaching rate of V and W reasonably well and that the optimal process conditions are reliable. The single-factor experiment can be used to determine the main influencing factors of the leaching rate and the optimum range for each factor. The response surface method is highly effective for investigating the significance of each factor and the interaction among various factors to optimize process conditions.

4. Conclusions

The pressure leaching of vanadium (V) and tungsten (W) in the spent SCR catalyst was optimized using Box-Behnken experimental design and the response surface analysis method. The effects of the leaching agent concentration, reaction temperature, and leaching time on the V and W leaching rate have been

investigated. Pressure alkaline leaching enabled the minimization of the concentration of leaching agent and time of leaching, thereby reducing the consumption of energy and material resources. By reducing the concentration of leaching agent and increasing the leaching temperature, we greatly shortened the leaching time and also improved the leaching efficiency. Moreover, while the reaction time and leaching temperature profoundly affected the V leaching rate, temperature and leaching agent concentration played a major role in determining the leaching rate of W. The excellent correlation was demonstrated between the predicted and measured values via the multivariate quadratic regression model. Thus it further indicates that the model is reliable for the recovery of metals from spent SCR catalysts via pressure alkaline leaching. Our study provides further knowledge of applying novel strategies for efficient recovery of metals by extensive utilization of spent catalysts.

Acknowledgements

This work was supported by National Water Pollution Control and Management Technology Major Projects (2014ZX07201-009-04), and "123 Project" of Environmental Research and Education in Liaoning Province (CEPF2013-123-1-4).

References

ANGELIDIS, T., TOURASANIDIS, E., MARINOU, E., STALIDIS, G., 1995. *Selective dissolution of critical metals from diesel and naptha spent hydrodesulphurization catalysts.* Resources, conservation and recycling. 13 (3-4), 269-282.

BORRA, C. R., BLANPAIN, B., PONTIKES, Y., BINNEMANS, K., VAN Gerven, T., 2016. *Recovery of rare earths and other valuable metals from bauxite residue (red mud): a review.* Journal of Sustainable Metallurgy. 2 (4), 365-386.

CHEN, G., WANG, J., WANG, X., ZHENG, S.-L., Du, H., ZHANG, Y., 2013. *An investigation on the kinetics of chromium dissolution from Philippine chromite ore at high oxygen pressure in KOH sub-molten salt solution.* Hydrometallurgy. 139, 46-53.

FAN, Y., YANG, Y., XIAO, Y., ZHAO, Z., LEI, Y., 2013. *Recovery of tellurium from high tellurium-bearing materials by alkaline pressure leaching process: Thermodynamic evaluation and experimental study.* Hydrometallurgy. 139, 95-99.

GHARBI, A., KENNÉ, J. P., 2000. *Production and preventive maintenance rates control for a manufacturing system: an experimental design approach.* International journal of production economics. 65 (3), 275-287.

GUO, L., SHU, Y., GAO, J., 2012. *Present and future development of flue gas control technology of DeNO_X in the world.* Energy Procedia. 17, 397-403.

HUO, Y., CHANG, Z., LI, W., LIU, S., DONG, B., 2015. *Reuse and valorization of vanadium and tungsten from waste V 2 O 5–WO 3/TiO 2 SCR catalyst.* Waste and Biomass Valorization. 6 (2), 159-165.

KENNÉ, J. P., 1999. *Experimental design in production and maintenance control problem of a single machine, single product manufacturing system.* International Journal of Production Research. 37 (3), 621-637.

KHURI, A. I., MUKHOPADHYAY, S., 2010. *Response surface methodology.* Wiley Interdisciplinary Reviews: Computational Statistics. 2 (2), 128-149.

KIM, J. W., LEE, W. G., HWANG, I. S., LEE, J. Y., HAN, C., 2015. *Recovery of tungsten from spent selective catalytic reduction catalysts by pressure leaching.* Journal of Industrial and Engineering Chemistry. 28, 73-77.

KU, H., JUNG, Y., JO, M., PARK, S., KIM, S., YANG, D., RHEE, K., AN, E.-M., SOHN, J., KWON, K., 2016. *Recycling of spent lithium-ion battery cathode materials by ammoniacal leaching.* Journal of hazardous materials. 313, 138-146.

LI, H.-Y., FANG, H.-X., WANG, K., ZHOU, W., YANG, Z., YAN, X.-M., GE, W.-S., LI, Q.-W., XIE, B., 2015. *Asynchronous extraction of vanadium and chromium from vanadium slag by stepwise sodium roasting–water leaching.* Hydrometallurgy. 156, 124-135.

LI, M., ZHENG, S., LIU, B., WANG, S., DREISINGER, D., ZHANG, Y., DU, H., ZHANG, Y., 2017. *A clean and efficient method for recovery of vanadium from vanadium slag: nonsalt roasting and ammonium carbonate leaching processes.* Mineral Processing and Extractive Metallurgy Review. 38 (4), 228-237.

LI, M.-T., CHANG, W., GANG, F., LI, C.-X., DENG, Z.-G., LI, X.-B., 2010. *Pressure acid leaching of black shale for extraction of vanadium.* Transactions of Nonferrous Metals Society of China. 20, s112-s117.

LI, Q., LIU, Z., LIU, Q., 2014. *Kinetics of Vanadium Leaching from a Spent Industrial V2O5/TiO2 Catalyst by Sulfuric Acid.* Industrial & Engineering Chemistry Research. 53 (8), 2956-2962.

LIU, Z. X., YIN, Z. L., XIONG, S. F., CHEN, Y. G., CHEN, Q. Y., 2014. *Leaching and kinetic modeling of calcareous bornite in ammonia ammonium sulfate solution with sodium persulfate.* Hydrometallurgy. 144, 86-90.

MAKADIA, A. J., NANAVATI, J., 2013. *Optimisation of machining parameters for turning operations based on response surface methodology.* Measurement. 46 (4), 1521-1529.

MARAFI, M., STANISLAUS, A., 2008. *Spent hydroprocessing catalyst management: A review: Part II. Advances in metal recovery and safe disposal methods.* Resources, Conservation and Recycling. 53 (1), 1-26.

MIRAZIMI, S., RASHCHI, F., SABA, M., 2013. *Vanadium removal from roasted LD converter slag: optimization of parameters by response surface methodology (RSM).* Separation and Purification Technology. 116, 175-183.

MUTHUKUMAR, M., MOHAN, D., RAJENDRAN, M., 2003. *Optimization of mix proportions of mineral aggregates using Box Behnken design of experiments.* Cement and Concrete Composites. 25 (7), 751-758.

MYERS, R. H., MONTGOMERY, D. C., ANDERSON-Cook, C. M., 2016. *Response surface methodology: process and product optimization using designed experiments.* John Wiley & Sons: 2016.

OOI, T. Y., YONG, E. L., DIN, M. F. M., REZANIA, S., AMINUDIN, E., CHELLIAPAN, S., RAHMAN, A. A., PARK, J., 2018. *Optimization of aluminium recovery from water treatment sludge using Response Surface Methodology.* Journal of environmental management. 228, 13-19.

PEREZ, J. P. H., FOLENS, K., LEUS, K., VANHAECKE, F., VAN DER Voort, P., DU LAING, G., 2019. *Progress in hydrometallurgical technologies to recover critical raw materials and precious metals from low-concentrated streams.* Resources, Conservation and Recycling. 142, 177-188.

QIU, S., WEI, C., LI, M., ZHOU, X., LI, C., DENG, Z., 2011. *Dissolution kinetics of vanadium trioxide at high pressure in sodium hydroxide–oxygen systems.* Hydrometallurgy. 105 (3-4), 350-354.

SHANG, X., HU, G., HE, C., ZHAO, J., ZHANG, F., XU, Y., ZHANG, Y., LI, J., CHEN, J., 2012. *Regeneration of full-scale commercial honeycomb monolith catalyst (V2O5–WO3/TiO2) used in coal-fired power plant.* Journal of Industrial and Engineering Chemistry. 18 (1), 513-519.

SHI, S., LV, J., LIU, Q., NAN, F., FENG, J., XIE, S., 2018. *Optimized preparation of Phragmites australis activated carbon using the Box-Behnken method and desirability function to remove hydroquinone.* Ecotoxicology and environmental safety. 165, 411-422.

SKELLAND, A., LEE, J. M., 1981. *Drop size and continuous-phase mass transfer in agitated vessels.* AIChE Journal. 27 (1), 99-111.

SOLANKI, A. B., PARIKH, J. R., PARIKH, R. H., 2007. *Formulation and optimization of piroxicam proniosomes by 3-factor, 3-level Box-Behnken design.* AAPS PharmSciTech. 8 (4), 43.

TEFAS, L. R., TOMUȚĂ, I., ACHIM, M., VLASE, L., 2015. *Development and optimization of quercetin-loaded PLGA nanoparticles by experimental design.* Clujul Medical. 88 (2), 214.

TEKINDAL, M. A., BAYRAK, H., OZKAYA, B., GENÇ, Y., 2012. *Box-Behnken experimental design in factorial experiments: The importance of bread for nutrition and health.* Turkish Journal of Field Crops. 17 (2), 115-123.

TUNCUK, A., CIFTCI, H., AKCIL, A., OGNYANOVA, A., VEGLIÒ, F., 2009. *Experimental design and process analysis for acidic leaching of metal-rich glass wastes.* Waste Management & Research. 28 (5), 445-454.

WHITE, C. D., WILLIS, B. J., NARAYANAN, K., DUTTON, S. P., 2001. *Identifying and estimating significant geologic parameters with experimental design.* SPE Journal. 6 (03), 311-324.

YANG, J., MA, H., YAMAMOTO, Y., YU, J., XU, G., ZHANG, Z., SUZUKI, Y., 2013. *SCR catalyst coated on low-cost monolith support for flue gas denitration of industrial furnaces.* Chemical engineering journal. 230, 513-521.

ZHOU, X., WEI, C., XIA, W., LI, M., LI, C., DENG, Z., XU, H., 2012. *Dissolution kinetics and thermodynamic analysis of vanadium trioxide during pressure oxidation.* Rare Metals. 31 (3), 296-302.

ZI, W., PENG, J., ZHANG, X., ZHANG, L., LIU, J., 2013. *Optimization of waste tobacco stem expansion by microwave radiation for biomass material using response surface methodology.* Journal of the Taiwan Institute of Chemical Engineers. 44 (4), 678-685.